The 2013 World Congress on
Advances in Structural Engineering and Mechanics (ASEM13)
Jeju, Korea, September 8-12, 2013

Thermomechanical characterization of an Fe-Mn-Si-Cr-Ni-VC shape memory alloy for application in prestressed concrete structures

*W.J. Lee, B. Weber, G. Feltrin, M. Motavalli and C. Leinenbach

Empa, Swiss Federal Laboratories for Materials Science and Technology,
Überlandstrasse 129, CH-8600 Dübendorf, Switzerland
**wookjin.lee@empa.ch*

ABSTRACT

Fe-Mn-Si based shape memory alloys are a promising solution for advanced civil engineering applications such as post-tensioning elements in concrete structures, since they are cost-effective and show large and stable recovery stresses at ambient temperature compared to conventional NiTi shape memory alloys. In this paper, a detailed experimental evaluation of the thermo-mechanical properties of an Fe-Mn-Si-Cr-Ni-VC alloy has been carried out. The recovery behavior, prestressing effects, as well as the cyclic thermo-mechanical response after activating the prestressing force are investigated. The experimental results show the potential of the Fe-Mn-Si-Cr-Ni-VC alloy for a wide range of post-tensioning applications in concrete structures.

1. INTRODUCTION

Concrete has an excellent compressive strength but low tensile strength and low ductility. When concrete is subjected to tensile or bending stress, brittle fracture occurs since a concrete material normally does not undergo plastic deformation and cannot dissipate a high amount of energy before failure. To avoid this disadvantage and to improve the structural reliability of concrete structures, various kinds of advanced reinforcement types such as fiber reinforced concrete and prestressed concrete have been developed, which are widely used in civil engineering.

Shape memory alloy (SMA) steels based on the Fe-Mn-Si alloy system are promising candidates for a variety of advanced civil engineering applications, since they have a wide transformation hysteresis, high elastic stiffness and strength and are inexpensive to produce (Maruyama and Kubo, 2011). These advantages make them promising as a cost-effective alternative to conventional NiTi-based SMAs for applications requiring high shape memory stresses, e.g. constrained recovery applications such as external confinement for reinforced concrete columns (Choi et al., 2010) or as reinforcement in prestressed concrete (Czaderski et al., 2006; Maji and Negret, 1998).

Recently, some of the present authors reported that Fe-SMAs with finely dispersed VC particles have very promising properties for commercial civil engineering applications, in particular a very high recovery stress after heating to only 130°C (Dong et al., 2009; Leinenbach et al., 2012). These studies confirmed the high potential and cost efficiency of these Fe-SMAs for advanced civil engineering applications. However, before the Fe-SMAs can be widely accepted for civil applications, their thermo-mechanical behavior under realistic loading conditions needs to be investigated in detail. The experimental study presented in this paper aimed at evaluating some important thermo-mechanical properties of a recently developed Fe-SMA, which are required for its application in prestressed concrete structures. The recovery behavior and the prestressing effect of the alloy were studied for different pre-strain and heating conditions. The prestress loss by cyclic thermo-mechanical loading during operations was also investigated.

2. MATERIAL AND TEST SET UP

The alloy studied in the present work (Fe-17Mn-5Si-10Cr-4Ni-1(V,C) (ma-%)) was prepared by standard induction casting procedure under atmospheric conditions. The cylindrical ingot with 90 mm diameter and 300 mm height was then heated to 1100°C and hot pressed to 50 mm width, followed by stepwise reheating to 1100°C for 15 min and hot pressing down to a final thickness of 15 mm. After the hot pressing, the alloy was solution treated for 5 h at 1100°C and water quenched. Finally, an aging heat treatment was performed at 850°C for 2 h in a laboratory vacuum furnace. More details about the manufacturing process of the alloy can be found in (Leinenbach et al., 2012).

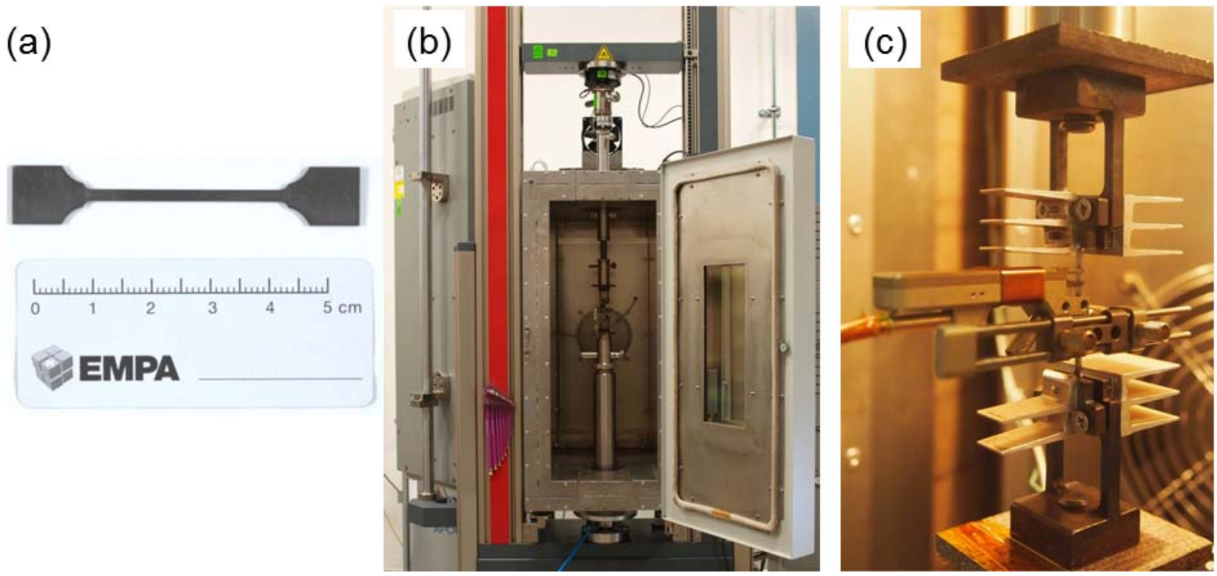

Fig. 1 (a) Geometry and dimension of the sample, (b) tensile testing machine with climate chamber and (c) clip-on extensometer.

For the experiments, dog-bone shaped tensile specimens with a gauge length of 32 mm and cross-section of 2·0.8 mm^2 were prepared using electro discharge machining (Fig. 1a). The thermo-mechanical tests were performed using a Zwick/Roell Z020 tensile testing machine containing a climate chamber, as shown in Fig. 1b. During the test, the strain evolution was measured with a clip-on extensometer with a gauge length of 20 mm (Fig. 1c). A thermocouple was tied to the extensometer to measure its temperature during the test in order to control the feedback as well as to compensate the errors resulted from the thermal expansion of the extensometer.

The samples were loaded and unloaded under strain-control at a deformation rate of 0.2 mm·min^{-1} . Heating and cooling of the samples was performed with a rate of 2°C·min^{-1}. For each heating or cooling step, the temperature of the chamber was kept constant for 20 min once the sample reached the desired temperature in order to achieve a homogeneous temperature distribution in the chamber.

In order to characterize the recovery behavior of the alloy, a tensile mechanical pre-strain in the range of 2 to 4 % was applied first. After the pre-straining, the samples were unloaded. A small tensile stress (σ = ~10 MPa) is imposed at the end of the unloading step in order to avoid gaps between the samples and the clamps of the test machine. The samples were then heated and cooled at two different conditions; (1) The free shape recovery behavior was investigated by measuring the strain evolution during heating and cooling under near-zero stress conditions. (2) The behavior of the recovery stress development was studied in a constrained heating test, i.e. heating and cooling of the sample while keeping the total length of the sample constant.

The cyclic mechanical behavior of the alloy was investigated by thermo-mechanical tests that comprised two stages: In the first stage, the recovery stress was generated following the same procedure as for the constrained heating tests. In the second stage, cyclic mechanical loading was applied after the generation of the recovery stress in the samples.

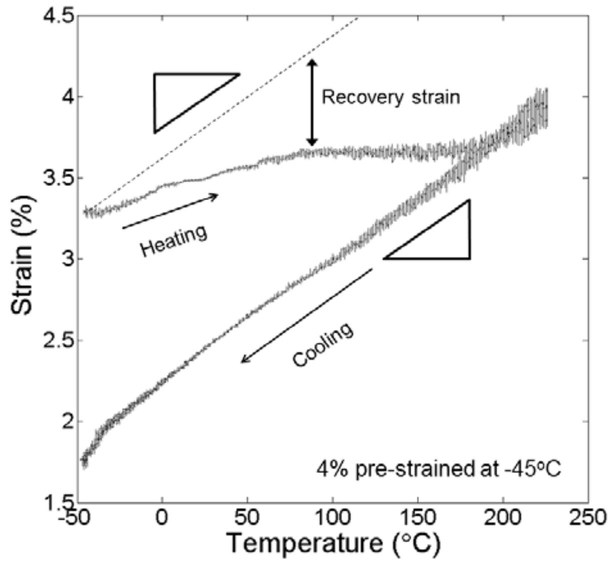

Fig. 2 Heating and cooling curve for the sample pre-strained to 4 % at -45°C.

3. RECOVERY BEHAVIOR

3.1 Free shape recovery behavior

After pre-straining and unloading, the residual pre-strain of the alloy is partially recovered when heating the sample. Previous studies with similar alloys showed that the amount of recovery strain depends significantly on the pre-strain (Kajiwara et al., 2001; Baruj et al., 2002; 2004) and the pre-strain temperature (Sato and Mori, 1991; Jian and Wayman, 1994; Dong et al., 2009). In this section, the effect of different pre-strain parameters, i.e. pre-strain and pre-strain temperature, on the recovery strain of the alloy is investigated.

Fig. 2 shows a typical heating and cooling curve for the pre-strained sample. It can be seen that the shape recovery took place during heating. For the sample which was deformed by 4 % at -45°C, approximately 1.6 % strain was recovered when the temperature reached 175°C, and above this temperature the sample showed normal thermal expansion.

Effect of pre-strain   Fig. 3a shows the recovery strain as a function of the pre-strain for samples deformed at room temperature (RT) and heated to 200°C. With increasing pre-strain, the recovery strain firstly increased linearly to a maximum value of 0.7 %, and then remained almost constant for pre-strains larger than 4 %.

Effect of pre-strain temperature   Fig. 3b shows the recovery strain as a function of the pre-strain temperature for samples deformed by 4 %. The result shows that the recovery strain depends strongly on the pre-strain temperature. The recovery strain decreased with pre-strain temperature from 1.6 % (-45°C) to 0.8 % (RT) and finally to 0.6 % (60°C).

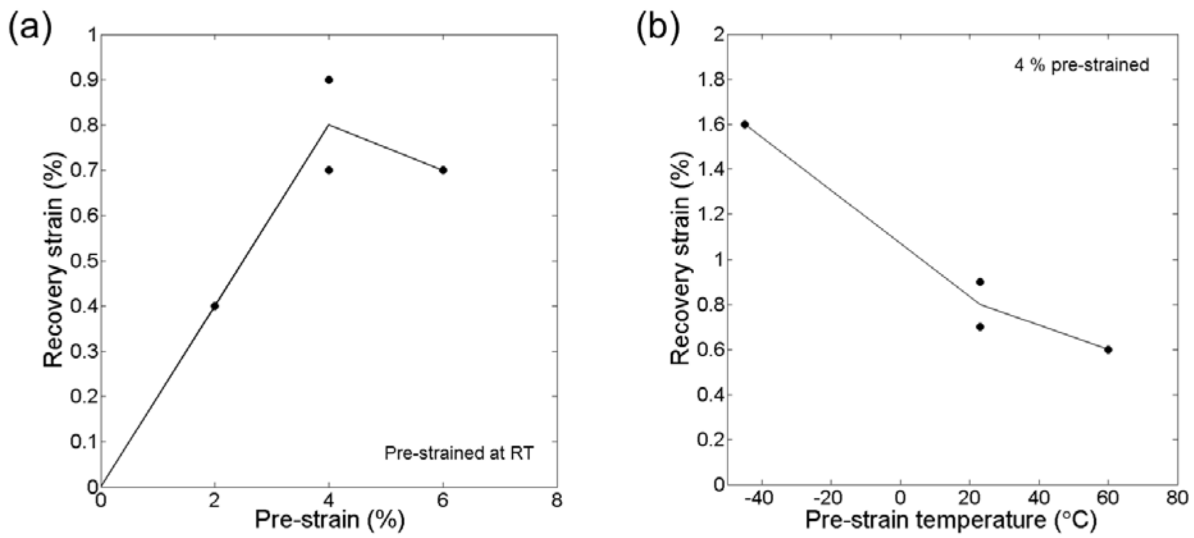

Fig. 3 Recovery strain as functions of (a) pre-strain and (b) pre-strain temperature.

3.2 Recovery stress

Constrained heating tests were carried out in order to estimate the level of prestress which can be generated in the alloy. For practical applications, electric resistance has been frequently used to heat up the SMA elements (Li et al., 2007; Choi et al., 2008). Since this process enables local heating of the SMA element without heating the whole structure, it has been assumed that the SMA is completely constrained during activating the prestress. This condition was considered in the experiment by keeping the total length of the sample constant during the heating and cooling steps.

Fig. 4 presents a typical recovery stress-temperature curve of the alloy. The curve was obtained with a sample pre-strained to 4 % and heated to 140°C. The development of the recovery stress started almost instantaneously with the onset of heating and continued throughout the entire heating step, showing a positive linear correlation between the temperature and the stress upon the heating. In other words, the recovery stress increased with increasing the temperature, and reached about 130 MPa at 140°C. During cooling to RT, the recovery stress increased further due to the thermal contraction of the alloy.

Fig. 5a shows the final recovery stresses at RT after a heating and cooling step as a function of pre-strain temperature. The level of the final recovery stress was independent from the pre-strain temperature. As shown in the figure, the final recovery stresses were all around 400 MPa for all the samples independent from the pre-strain temperature, although the recovery strain depends significantly on the pre-strain temperature. Fig. 5b shows the final recovery stresses as a function of the heating temperature for two different pre-strains of 2 % and 4 %. The level of stress increased when increasing the heating temperature. When increasing the pre-strain from 2 % to 4 %, the stress also increased slightly. The highest recovery stress of 400 MPa was obtained after applying a pre-strain of 4 % and heating to 160°C.

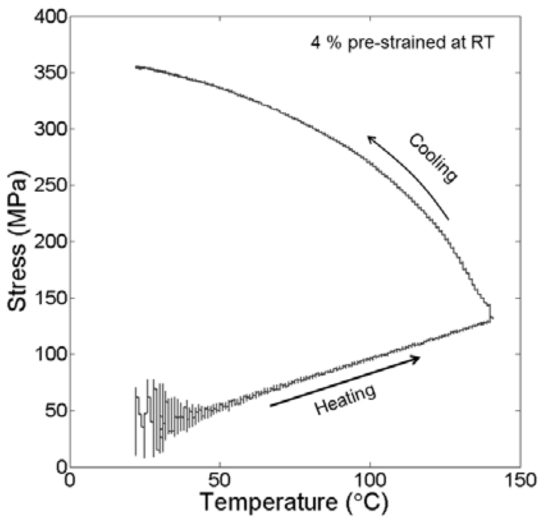

Fig. 4 Representative recovery stress curve of the alloy, with pre-strain of 4 % and heating temperature of 140°C.

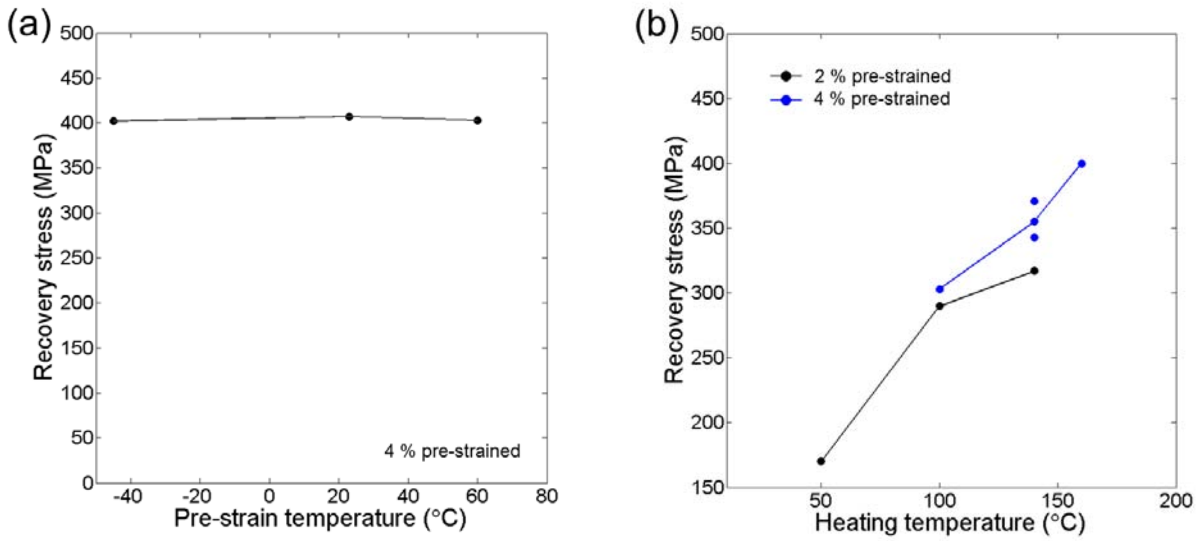

Fig. 5 (a) Effect of pre-strain temperature on final recovery stress and (b) recovery stress as a function of heating temperature for two different pre-strain levels.

3.3 Discussions

The experimental observations on the free recovery behavior show that the recovery strain of the alloy depends on many factors such as pre-strain, pre-strain temperature and heating temperature. However, it seems that the level of the final recovery stress does not solely depend on the possible amount of the recovery strain. For instance, the result in Fig. 3b shows that the recovery strain relies significantly on the pre-strain temperature. However, under conditions of the present work, the samples pre-strained at different temperatures showed the same levels of the final recovery stress when all the other parameters were the same.

In the cases of conventional NiTi- and NiTiNb-based alloys, relaxation of the recovery stress during cooling to RT has been observed, e.g. by Choi et al. (2010). However, the alloy studied here showed no stress relaxation during cooling and the stress increased continuously. As a result, the recovery stresses after cooling to ambient temperature were much higher than those reported for the NiTi- and NiTiNb-based alloys, which are generally less than 100 MPa (Choi et al. 2010). This behavior is beneficial for civil engineering applications where high recovery stress at ambient temperature is necessary for prestressing of the concrete structure.

In the constrained heating test, the final recovery stress at RT increased with increasing pre-strain and with increasing heating temperature. The highest recovery stress of 400 MPa was obtained when the pre-strain was 4 % and the heating temperature was 160°C. Based on the experimental results, the prestress which can be generated using the alloy in the application are estimated to be up to 400 MPa, depending on the maximum allowable temperature of the concrete structure.

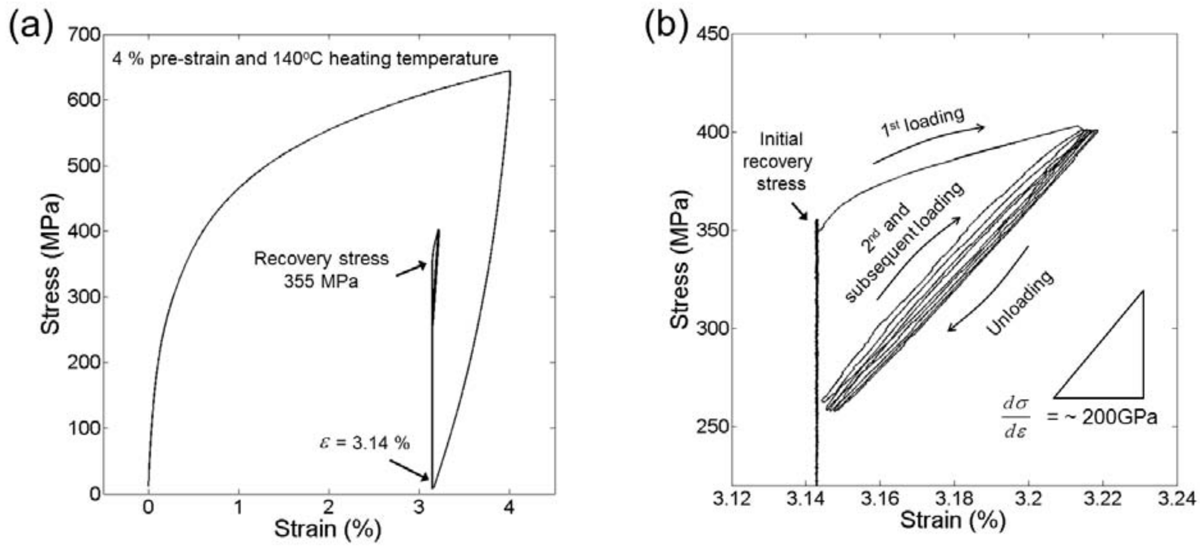

Fig. 6 Cyclic stress-strain curve of the alloy after generating the recovery stress with 4 % pre-strain and 140°C heating temperature. (a) For all steps of the cyclic test and (b) enlarged curve showing the cyclic behavior.

4. EFFECT OF CYCLIC LOADINGS ON PRESTRESSES

Since concrete structures are generally subjected to cyclic loading during operation, the cyclic mechanical behavior of the alloy in the prestressed state is one of the important factors that need to be considered for any application. In this regard, cyclic mechanical tests were carried out after a shape recovery stress was generated.

For the tests, samples were pre-strained to 4 % and the recovery stress was generated with a heating temperature of 140°C. After generating the recovery stress, the temperature was fixed at RT. The samples were then strained cyclically to 0.07 % and released to the original strain. This process was repeated 5 times.

Fig. 6a illustrates the stress-strain behavior of a sample during the cyclic test. Heating and cooling of the sample was done while keeping the strain of the sample at ~3.14 %. After heating, a final recovery stress of 355 MPa was obtained. Fig. 6b provides a closer look at the cyclic test result presented in Fig. 6a. The loading step of the first cycle results in an inelastic deformation, while the unloading is linear. This leads to a reduction of the recovery stress to 262 MPa. In the subsequent cycles, the alloy behaves linearly and the recovery stress remains stable. The slope of the stress-strain loops from the second to the fifth cycle was approximately 200 GPa and corresponded well with the elastic modulus of the steel, which is generally in the range of 180 to 220 GPa.

The results presented in Fig. 6 indicate that the possible recovery stress loss is about 25 % of the total recovery stress even under an extreme cyclic loading, i.e. for a 0.07 % strain cycle and return to the initial strain. It is worth noting that this test scenario do not accurately represent the true prestress losses by the cyclic external load in a prestressed concrete structure. Recently, Shin and Andrawer (2011) and

Dommer and Andrawes (2012) conducted experiments for evaluating prestress changes during loading and unloading cycles of concrete columns retrofitted with NiTiNb SMA wires. Their results showed that the SMA wire does not return to the initial position after loading and unloading cycle of the column even when there is no damage during loading in the concrete, due to the volumetric changes of the concrete induced by different prestress state. It is therefore expected that typical external loads on the prestressed concrete have less impact on the level of recovery stress losses in the alloy.

5. SUMMARY AND OUTLOOK

This paper accesses the thermo-mechanical properties of an Fe-based SMA for reinforcing elements in a prestressed concrete structure. The alloy used for the study was Fe–17Mn–5Si–10Cr–4Ni with 1% VC precipitates, which is a relatively new type of alloy that has potential in civil structural applications.

It is shown that the recovery stress of the alloy relies mainly on the heating temperature and the pre-strain. The alloy can produce stable prestresses up to 400 MPa at RT after pre-straining to 4 % and heating to 160°C. This level of recovery stress is much higher than those reported for NiTi- and NiTiNb-based alloys, which are generally less than 100 MPa at RT, and other Fe-based SMAs, which are in the range of 250-350 MPa (Dong et al, 2005).

Interestingly, the effect of the pre-strain temperature on the recovery stress was negligible although the recovery strain depends significantly on this factor. To understand this phenomenon, further study including detailed investigations of phase transformations in the alloy may be necessary.

The cyclic tests indicated that the prestressed alloy undergoes plastic deformation during the first mechanical loading. Thus the first loading cycle may lead to a prestress loss in the concrete structure. On the other hand, after the first cycle the alloy behaved elastically and the level of stress remained stable on subsequent cycles. When applying a 0.07 % strain and returning to the initial strain, the recovery stress dropped from 355 MPa to 290 MPa. However, when considering the fact that the SMA does not return to the initial position after loading and unloading cycle in the prestressed concrete, it is expected that typical external loads on the prestressed concrete have less impact on the level of recovery stress losses in the alloy.

In conclusion, it is strongly believed that the Fe-based SMA studied here is suitable for prestressed concrete applications. Since the alloy is very cost effective in comparison with conventional NiTi-based alloys and can easily produce high prestressing forces without any hydraulic devices, this alloy is likely to be competitive for prestressing of concrete structures when compared to conventional steel or SMA reinforcing elements.

REFERENCES

Baruj A, Kikuchi T, Kajiwara S and Shinya N. (2002) "Effect of Pre-Deformation of Austenite on Shape Memory Properties in Fe-Mn-Si-based Alloys Containing Nb and C". *Mater. Trans*., **43(3)**, 585-588.

Baruj A, Kikuchi T, Kajiwara S and Shinya N. (2004) "Improvement of shape memory properties of NbC containing Fe–Mn–Si based shape memory alloys by simple thermomechanical treatments". *Mater. Sci. Eng. A.*, **378**, 333-336.

Choi E, Nam TH, Cho SC, Chung YS and Park T. (2008) "The behavior of concrete cylinders confined by shape memory alloy wires". *Smart Mater. Struct.*, **17**: 1-10.

Choi E, Chung Y-S, Choi J-H, Kim H-T and Lee H. (2010) "The confining effectiveness of NiTiNb and NiTi SMA wire jackets for concrete". *Smart Mater. Struct.,* **19**, 1–8.

Czaderski C, Hahnebach B and Motavalli M (2006) "RC beam with variable stiffness and strength". *Construction Building Mater.,* **20**, 824–833.

Dommer K and Andrawes B. (2012) "Thermomechanical characterization of NiTiNb shape memory alloy for concrete active confinement applications". *J. Mater. Civil Eng.*, 24(10): 1274-1282.

Dong Z, Klotz UE, Leinenbach C, Bergamini A, Czaderski C and Motavalli M. (2009) "A novel Fe-Mn-Si shape memory alloy with improved shape recovery properties by VC precipitation". *Adv. Eng. Mater.,* **11**, 40-44.

Jian L and Wayman CM. (1994) "Shape memory effect and related phenomena in a microalloyed Fe-Mn-Si alloy". *Mater. Charac.*, **32**, 215-227.

Kajiwara S, Liu D, Kikuchi T and Shinya N. (2001) "Remarkable improvement of shape memory effect in Fe-Mn-Si based shape memory alloys by producing NbC precipitates". *Scripta Mater.*, **44**, 2809-2814.

Leinenbach C, Kramer H, Bernhard C and Eifler D. (2012), "Thermo-mechanical properties of an Fe-Mn-Si-Cr-Ni-VC shape memory alloy with low transformation temperature". *Adv. Eng. Mater.,* **14**, 62-67.

Li L, Li Q and Zhang F. (2007) "Behavior of smart concrete beams with embedded shape memory alloy bundles". *J. Intelligent Mater. Sys. Struct.*, **18**, 1003-1014.

Maji KA and Negret I (1998) "Smart prestressing with shape memory alloy". *J. Eng. Mech.*, **124(10)**: 1121–1128.

Maruyama T, Kubo K. (2011) "Ferrous (Fe-based) shape memory alloys (SMAs): properties, processing and applications", in Yamauchi K, Ohkata I, Tsuchiya K, Miyazaki S. (eds.), *"Shape Memory and Superelastic Alloys: Technologies and Applications".,* Woodhead Publishing LTD., Cambridge, p141-159.

Sato A and Mori T. (1991) "Development of a shape memory alloy Fe-Mn-Si". *Mater. Sci. Eng. A.*, **146**, 197-204.

Shin M and Andrawes B. (2011) "Emergency repair of severely damaged reinforced concrete columns using active confinement with shape memory alloys". *Smart Mater. and Struct.*, **20(6)**, 1-9.